IOPscience iopscience.iop.org

Home Search Collections Journals About Contact us My IOPscience

Memory effect in an ionic liquid matrix containing single-walled carbon nanotubes and polystyrene

This content has been downloaded from IOPscience. Please scroll down to see the full text.

2008 Nanotechnology 19 055203

(http://iopscience.iop.org/0957-4484/19/5/055203)

View the table of contents for this issue, or go to the journal homepage for more

Download details:

IP Address: 141.211.4.224
This content was downloaded on 10/09/2015 at 22:30

Please note that terms and conditions apply.

Nanotechnology 19 (2008) 055203 (4pp) doi:10.1088/0957-4484/19/05/055203

Memory effect in an ionic liquid matrix containing single-walled carbon nanotubes and polystyrene

Di Wei[1,4], Jayanta K Baral[2,3], Ronald Österbacka[2] and Ari Ivaska[1]

[1] Process Chemistry Centre, c/o Laboratory of Analytical Chemistry, Åbo Akademi University, Biskopsgatan 8, FIN-20500 Åbo/Turku, Finland
[2] Centre for Functional Materials, c/o Department of Physics, Åbo Akademi University, Porthansgatan 3, FIN-20500 Åbo/Turku, Finland
[3] Graduate School of Materials Research, Universities of Turku, Turku, Finland
[4] Centre of Advanced Photonics and Electronics, Department of Engineering, University of Cambridge, 9 J J Thomson Avenue, Cambridge CB3 0FA, UK

E-mail: dw344@ cam.ac.uk

Received 15 August 2007, in final form 25 November 2007
Published 14 January 2008
Online at stacks.iop.org/Nano/19/055203

Abstract
We report the use of an ionic liquid (IL) gel matrix containing a blend of single-walled carbon nanotubes (SWNTs) and polystyrene (PS) as a memory device. SWNTs and PS beads were mixed in a room-temperature IL, 1-butyl-3-methyl-hexafluorophosphate ([BMIM][PF_6]). The composite gel was sandwiched between a bottom ITO glass and a top aluminium electrode. By merely changing the concentrations of SWNTs in the inert insulating PS matrix, we observed several distinct electrical properties of the device, such as an insulator, a memory in terms of switching and negative differential resistance (NDR), and a conductor. The electric bistable switching hops between a higher impedance (OFF) state and a lower impedance (ON) state which is approximately equal to five orders of current decays.

(Some figures in this article are in colour only in the electronic version)

1. Introduction

Carbon nanotubes have attracted intensive attention for their extraordinary mechanical and electronic properties. Non-volatile random access memory for molecular computing based on carbon nanotubes was proposed in 2000 [1]. Since then, memory devices based on multi-walled carbon nanotubes (MWNTs) and single-walled carbon nanotubes (SWNTs) have begun to be reported.

Non-volatile memory devices made of MWNTs can be built based on electrostatic telescoping [2, 3]. The electrostatic forces are induced by the voltage differences in the binding energy between the carbon nanotube (CNT) and metal electrodes. Inner CNTs of a MWNT can be extracted by the electrostatic force. The material of the metal electrode should be carefully chosen to achieve the non-volatility of this memory. Memory devices composed of SWNTs have also been reported recently. Different strategies of using SWNTs in memory devices based on hysteresis effect, floating gate, etc, have been proposed [4–12]. Two-bit memory devices made of SWNTs were reported and the pertinent memory behaviours were supposed to originate from the capacitive effect due to polarization of the solvent molecules (e.g. H_2O) [12]. However, most memory effect studies are focused on a single SWNT. From the practical application point of view, it is hard to currently manufacture devices based on finely ordered single SWNTs. Here, we demonstrate multifunction devices based on an ionic liquid (IL) matrix containing SWNTs and polystyrene (PS).

Carbon nanotubes can be functionalized with PS by various methods [13, 14]. Dispersing SWNTs into PS was reported to improve the electrical conductivity and mechanical properties of the composite material [15–17]. In this paper, both PS and SWNTs are simply mixed together in the IL gel. By merely tuning the concentration of SWNTs, the device shows several distinct electrical behaviours ranging from insulator or memory device to conductor.

 © 2008 IOP Publishing Ltd Printed in the UK

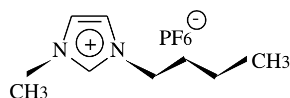

Scheme 1. The chemical structure of the ionic liquid 1-butyl-3-methyl-imidazolium hexafluorophosphate ([BMIM][PF_6]).

2. Experiments

1-butyl-3-methyl-hexafluorophosphate ([BMIM][PF_6]) (⩾98%) was bought from Solvent Innovation and the structure was shown in scheme 1.

PS beads (⩾ 99%) were obtained from Aldrich. SWNTs were purchased from Nanoport Co. Ltd (Shengzhen, China) with inner diameter <2 nm and length 5–15 μm. They were purified by refluxing in 3 M HNO_3 for 48 h, and then filtered through a 0.45 μm pore size nylon membrane with the aid of a pump and thoroughly washed with deionized water (ELGA, 18.2 MΩ cm). The materials were then dried under vacuum at 60 °C for 12 h before use. The purified SWNTs were ground in [BMIM][PF_6] for 10 min and then PS beads were added and ground for another 10 min. Adjusting the concentration of SWNTs and PS beads, three devices were fabricated for comparison. In order to understand which device is showing memory behaviour in terms of impedance switching and NDR, a set of three devices were fabricated on ITO as an ITO/IL_SWNT/Al device (4.5% SWCNT (wt%)), an ITO/IL_PS/Al device (7.3% PS (wt%)) and an ITO/IL_PS:SWNTs/Al device (4.2% SWNT, 6.9% PS (wt%)) in a [BMIM][PF_6] matrix. The IL gel was drop cast onto the ITO glass surface and dried in vacuum with heating at 60 °C under a vacuum of 1×10^{-6} mbar for 24 h. A layer of Al with a thickness of 50 nm was evaporated under a vacuum of ca. 1×10^{-6} mbar on top of the composite gel film at a uniform rate of evaporation (1.0–1.2 Å s^{-1}) to avoid Al penetration into the active medium. The thickness of the thermally evaporated Al electrode was measured by a thickness monitor TM-100 from MAXTEK, INC. Electrical characterization of the devices was performed by using a Keithley 2400 programmable voltage source meter and a Keithley 617 programmable electrometer or an Agilent 4142B modular DC source/monitor. Positive and negative bias was applied to the bottom ITO and the top Al electrodes, respectively. All electrical experiments were conducted inside a nitrogen-filled mBraun glove box. The structure of the device is shown in scheme 2.

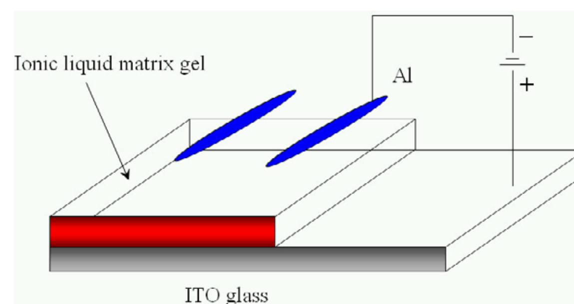

Scheme 2. Schematic structure of the device.

3. Results and discussion

The morphology of SWNTs and the gels were studied by a scanning electron microscope (SEM), which was from Leica Cambridge Instruments. The SEM pictures show that the SWNTs were embedded in the IL matrix (figure 1(c)) and, after being ground with PS, SWNTs are embedded inside the whole polymer–IL matrix (figure 1(d)).

To verify the interaction between the SWNTs and PS, the gels were characterized by Raman spectroscopy. The excitation wavelength of 780 nm (Renishaw, NIR diode laser) was used for the Raman measurements. The spectra are shown in figure 2 where (a) is the Raman spectrum of the purified SWNTs, (b) for the SWNTs mixing with the IL (4.52% SWNT), (c) for the mixture of SWCNT:PS (4.2% SWNT, 6.9% PS) in IL, (d) for the PS in IL (7.3%), (e) for the pure PS bead and (f) for the ITO glass.

The D band intensity versus the G band intensity (I_D/I_G) in figure 2(a) is around 0.26 and that in figure 2(b) is around 0.31. The small increase may be due to π–π interaction between the aromatic cation of IL and the SWNTs. I_D/I_G is still around 0.3 in figure 2(c), which means that there is no covalent bonding between the PS and SWNTs [13, 14]. Comparing figures 2(c)–(e), the peaks at 1159 and 992 cm^{-1} in figure 2(c) must be from PS and they are due to the benzene ring breathing [18]. The peak at 1573 cm^{-1} is due to the C=C stretching [18]. Since the gel from PS in IL (7.3%) is rather transparent, the increasing absorption at 1409 cm^{-1} in figure 2(d) should be due to the absorption of ITO glasses, as figure 2(f) proves.

The thickness of the three samples is determined by charge extraction in a linearly increasing voltage (CELIV) measurement. The detailed description of using CELIV for the thickness determination is given in [19]. The thickness of the active layer in the (a) ITO/IL_PS/Al device, (b) ITO/IL_PS:SWNTs/Al device and (c) ITO/IL_SWNT/Al device is ca. 500, 990 and 800 nm, respectively. The current density–voltage (J–V) characteristics of the (a) ITO/IL_PS/Al, (b) ITO/IL_PS:SWNTs/Al and (c) ITO/IL_SWNT/Al devices are shown in figure 3.

In a typical current density–voltage (J–V) characterization operated inside a nitrogen-filled mBraun glove box, the hysteresis of the devices has been illustrated in figure 3(b). When the ITO/IL_PS:SWNTs/Al device was scanned at a rate of 100 mV s^{-1} through the voltage sequence 0 V to +3 V, +3 to −3 V and −3 V to 0 V, as illustrated by the closed circles (●) shown in figure 3(b), the device is initially in a higher impedance or lower conductance (OFF) state, and above a given voltage threshold (V_{th}) it abruptly commutes to a much lower impedance or higher conductance (ON) state (V_{th} is close to 2.8 V here). The difference between the 'OFF' and 'ON' states, i.e. the current density jump, covers several current decades, approximately from 3 to 5. These low impedance states remain effective even when the device bias is swept back, thereby creating a hysteresis in the J–V curve. It is only when the voltage crosses zero or a voltage close to zero that the device is reset to the higher impedance state. Then, in the negative bias range one observes a curve quantitatively similar to

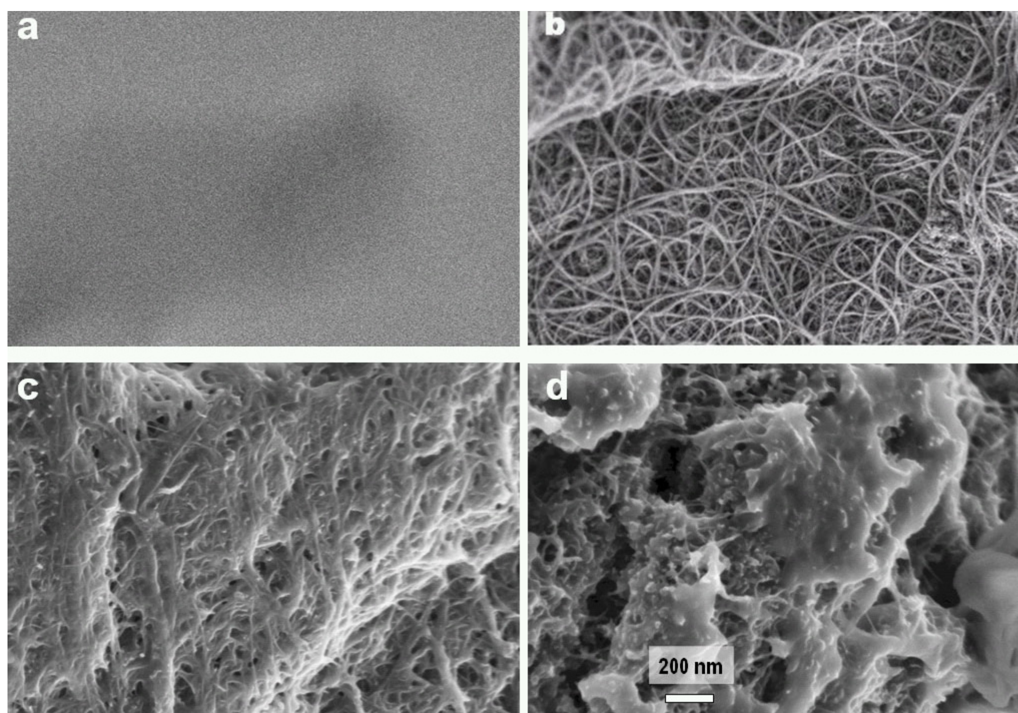

Figure 1. SEM of (a) IL_PS on ITO (7.3% PS, wt%), (b) purified SWNTs, (c) IL_SWNTs (4.5% SWNT, wt%), (d) IL_ SWCNT:PS (4.2% SWNT, 6.9% PS, wt%).

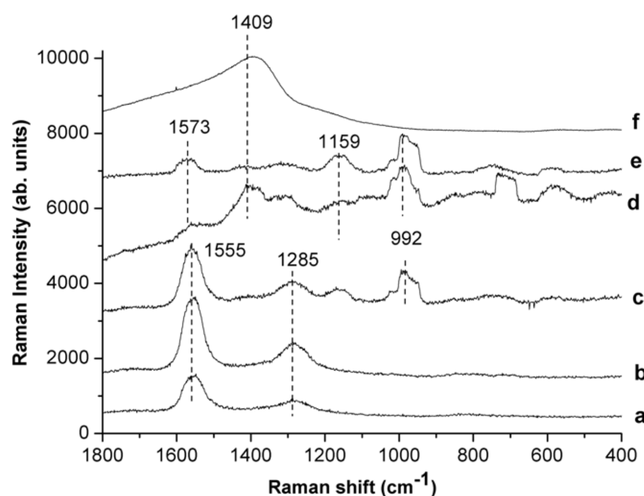

Figure 2. Raman spectrum (a) of the purified SWNTs, (b) of the SWNTs mixing with the IL (4.5% SWNT, wt%), (c) of the mixture of SWCNT:PS (4.2% SWNT, 6.9% PS, wt%) in IL, (d) of the PS in IL (7.3%, wt%), (e) of pure PS beads, and (f) of ITO glass. Spectra are shown with a shift in the baseline to improve the visualization.

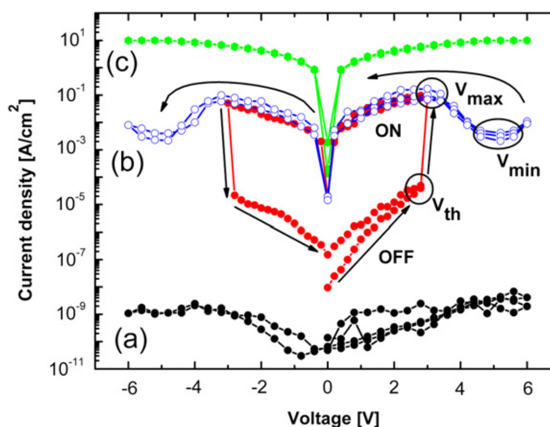

Figure 3. Current density (J) versus voltage (V) plot of the (a) ITO/IL_PS/Al device, (b) ITO/IL_PS:SWNTs/Al device and (c) ITO/IL_SWNT/Al device. The arrow represents the pathway of the current in different bias scan directions to get into bistability and NDR and the ON state. The threshold voltage (V_{th}), maximum voltage (V_{max}) and minimum voltage (V_{min}) are also shown.

that of the positive bias, with a sudden current jump to a lower impedance state, which remains effective until the device bias is swept back to zero. This transition of the device from OFF state to ON state is called bistability. The bistable behaviour of this device was observed when repeating the voltage cycle over again. However, after bias scanning this device five times, the impedance switching has gradually disappeared. The bistability may originate from the IL which helps to increase the conductivity of the device abruptly at threshold voltage. However, due to the over-oxidation/redox process inside the bulk of IL, the oxidized ionic liquid cannot irreversibly return to its neutral state and the device gradually loses its bistability. After disappearance of bistability, when the device was further scanned at a higher bias sequence from 0 to 6 V, 6 to −6 V and −6 V back to 0 V at the same scan rate of 100 mV s^{-1}, the region of negative differential resistance (NDR) was found between 3 and 6 V which is denoted by the open circles (○), as shown in figure 2(b), where current decreases with increasing voltage. There are several unique features noticeable

in this state, such as the observation of a local current maximum at V_{max} and a local current minimum at V_{min}. This J–V curve is called 'N-shaped' NDR [20]. The impedance switching and NDR memory properties could be very useful from the printable electronics point of view. A memory effect has been observed in thin films of insulating polymer and C_{60} nanocomposites [20–22]. Similar to our previous memory device mixing C_{60} with PS [20], which only shows 40% reproducibility of switching, the mixture of SWNTs in IL matrix containing PS shows bistability around 50% reproducibility for all the measurements. However, the reproducibility of NDR is 100% for all the measurements in our device made of the PS-IL matrix containing SWNTs. There are different models explaining the switching and NDR effect. Tang *et al* attributed the switching and NDR as general phenomena from nucleation of evaporated metal nanoislands formed in crevices created in the vicinity of dust particles and/or other impurities on the bottom electrode [23]. Majumdar *et al* suggested that tunnelling through 'metal-like' filaments within the bulk of the device is more probable for the anomalous current–voltage behaviour in the single-layer sandwich device [24]. The electronic properties of the SWNTs vary in a periodic way from metallic to semiconductor as a function of both diameter and helicity. It has been shown that 1/3 of SWNTs are metallic while the others are semiconducting with a bandgap inversely proportional to the diameter [25]. In this case, the NDR may be attributed to electron hopping between the isolated metallic conducting SWNTs in the insulating matrix.

In order to understand which device is showing memory behaviour in terms of impedance switching NDR, two other devices (ITO/IL_PS/Al and ITO/IL_SWNT/Al) are characterized. All the parameters of the electronic characterization were kept the same. They were also scanned under the bias sequence 0 to +6 V, +6 to −6 V and −6 V back to 0 V at the same scan rate of 100 mV s^{-1}. Neither bistability nor NDR has been observed in both of the above devices. The J–V characteristics of the ITO/IL_PS/Al and ITO/IL_SWNT/Al devices have been represented in figures 3(a) and (c), respectively. The ITO/IL_PS/Al device behaves like an insulator, whereas the ITO/IL_SWNT/Al device behaves like a conductor. Hence we have concluded that the memory behaviour in terms of impedance switching and NDR has been only from the SWCNT:PS device where SWCNTs were dispersed inside the inert polymer PS matrix. Thus NDR in our device may be due to the hopping of electrons between the metallic SWNTs, which are embedded in the matrix of insulating PS, and the semiconducting SWNTs in ILs. Use of NDR as a memory element in electronic devices had been reported earlier [26].

4. Conclusions

In conclusion, we have reported a simple fabrication method to produce IL-based memory devices containing SWNTs and PS where the programming of a continuum of states is possible through the use of applied bias above the critical threshold voltage V_{th}. The impedance states for NDR are non-volatile in nature and can be read and switched several times inside a nitrogen-filled mBraun glove box.

When the mechanism behind the switching effect and existence of multistable impedance states are well understood, an easily fabricated, high-density, low-cost and reliable data storage device can be optimized for practical applications.

Acknowledgments

This work is part of the activities of the Åbo Akademi Process Chemistry Centre within the Finnish Centre of Excellence Program (2000–2011) supported by the Academy of Finland and TEKES FinNano Program from the Department of Physics.

References

[1] Rueckes T, Kim K, Joselevich E, Tseng G Y, Cheung C L and Lieber C M 2000 *Science* **289** 94
[2] Kang J W and Jiang Q 2007 *Nanotechnology* **18** 095705
[3] Deshpande V V, Chiu H Y, Postma H W Ch, Miko C, Forro L and Bockrath M 2006 *Nano Lett.* **6** 1092
[4] Fuhrer M S, Kim B M, Durkop T and Brintlinger T 2002 *Nano Lett.* **2** 755
[5] Ganguly U, Kan E C and Zhang Y 2005 *Appl. Phys. Lett.* **87** 043108
[6] Choi W B, Chae S, Bae E, Lee J W, Cheong B H, Kim J R and Kim J J 2003 *Appl. Phys. Lett.* **82** 275
[7] Cui J B, Sordan R, Burghard M and Kern K 2002 *Appl. Phys. Lett.* **81** 3260
[8] Hollingsworth J P and Bandaru P R 2005 *Appl. Phys. Lett.* **87** 233115
[9] Lu X B and Dai J Y 2006 *Appl. Phys. Lett.* **88** 113104
[10] Radosavljevic M, Freitag M, Thadani K V and Johnson A T 2002 *Nano Lett.* **2** 761
[11] Marty L, Bonnot A M, Bonhomme A, Iaia A, Naud C, Andre E and Bouchiat V 2006 *Small* **2** 110
[12] Guo A, Fu Y, Wang C, Guan L, Liu J, Shi Z, Gu Z, Huang R and Zhang X 2007 *Nanotechnology* **18** 125206
[13] Li H, Cheng F, Duft A M and Adronov A 2005 *J. Am. Chem. Soc.* **127** 14518
[14] Wu H, Tong R, Qiu X, Yang H, Lin Y, Cai R and Qian S 2007 *Carbon* **45** 152
[15] Chang T, Kisliuk A, Rhodes S M, Brittain W J and Sokolov A P 2006 *Polymer* **47** 7740
[16] Putz K, Krishnamoorti R and Green P F 2007 *Polymer* **48** 3540
[17] Xie L, Xu F, Qiu F, Lu H and Yang Y 2007 *Macromolecules* **40** 3296
[18] Santos J C, Reis M M, Machado R A F, Bolzan A, Sayer C, Giudici R and Araujo P H H 2004 *Ind. Eng. Chem. Res.* **43** 7282
[19] Juska G, Arlauskas K, Viliunas M, Genevicius K, Osterbacka R and Stubb H 2000 *Phys. Rev.* B **62** R16235
[20] Majumdar H S, Baral J K, Österbacka R, Ikkala O and Stubb H 2005 *Org. Electron.* **6** 188
[21] Kanwal A and Chhowalla M 2006 *Appl. Phys. Lett.* **89** 203103
[22] Paul S, Kanwal A and Chhowalla M 2006 *Nanotechnology* **17** 145
[23] Tang W, Shi H, Xu G, Ong B S, Popovic Z D, Deng J, Zhao J and Rao G 2005 *Adv. Mater.* **17** 2307
[24] Majumdar H S, Baral J K, Laiho A, Ruokolainen J, Ikkala O and Osterbacka R 2006 *Adv. Mater.* **18** 2805
[25] Wildoer J W G, Venema L C, Rinzler A G, Smalley R E and Dekker C 1998 *Nature* **391** 59
[26] Nakasha Y and Watanabe Y 1995 Resonance tunnel diode memory *US Patent Specification* 5390145